Journal of Catalysis **190,** 296–308 (2000)
doi:10.1006/jcat.1999.2752, available online at http://www.idealibrary.com on IDEAL®

Evaluation of the Role of the Metal–Support Interfacial Centers in the Dry Reforming of Methane on Alumina-Supported Rhodium Catalysts

P. Ferreira-Aparicio,* M. Fernandez-Garcia,* A. Guerrero-Ruiz,† and I. Rodríguez-Ramos*

*Instituto de Catálisis y Petroleoquímica, C.S.I.C. Campus de Cantoblanco, 28049 Madrid, Spain; and †Departamento de Química Inorgánica y Técnica, U.N.E.D., C/ Senda del Rey, s/n, 28040 Madrid, Spain

Received July 14, 1999; revised September 24, 1999; accepted November 1, 1999

The reforming of CH_4 with CO_2 (dry reforming) has been studied on a series of Al_2O_3-supported Rh–Cu catalysts. The reaction has been found to proceed on these systems through a bifunctional mechanism, in which the activation on methane takes place on the rhodium phase while carbon dioxide is activated on the support surface via formate intermediates. The addition of a metal, such as copper, inactive for methane activation, has allowed us to evaluate the role of the interfacial Rh–Al_2O_3 sites in the reaction. The presence of copper reduces the stability of the catalysts, though it does not have any effect on the initial activity per surface exposed site. It indicates that the dry reforming of methane is not a structure-sensitive reaction and that catalytic activity, largely affected by the alumina support, is dependent on the number of surface exposed rhodium centers. © 2000 Academic Press

INTRODUCTION

The reforming of methane with carbon dioxide has received a great deal of attention during the past decade for two reasons (1). First, it is an interesting alternative for the revalorization of two of the most abundant and least expensive carbon-containing compounds. The reaction between these two raw materials yields synthesis gas ($H_2 + CO$), from which a wide variety of valuable hydrocarbons and oxygenates can be synthesized. Second, due to its high reaction enthalpy, it is an advantageous route for the storage of renewable energy sources, such as solar energy, with application in chemical energy transmission systems (2). Among the different catalysts studied for this process, rhodium-based catalysts exhibited the best behavior. An alumina-supported rhodium catalyst has been selected for the industrial application of the carbon dioxide reforming of methane for CO production, which has been commercialized as the Calcor process (3).

Several groups have stressed the influence of the support on the catalytic activity of a given metal, not only for methane activation (4, 5) but also for the dry reforming of methane (6–8). Nonsupported metals or metals supported on inert materials for this reaction, such as silica, show much lower levels of activity in terms of turnover numbers as compared with metals supported on alumina, titania, or zirconia (9). Mechanistic studies of these reactions indicate the participation of surface diffusion and spillover processes of hydrogen and oxygen species from the metal to the support and vice versa, justifying the above-mentioned observations. Bifunctional mechanisms in which methane is activated on the metal and carbon dioxide on the support have been often proposed for metals dispersed on oxidic supports, such as ZrO_2 (9–11), TiO_2 (6, 11, 12), or γ-Al_2O_3 (6, 13, 14). This kind of mechanism, in which two distinct types of active centers are involved in the reaction pathway, suggests two possibilities regarding the relative location of these sites: (a) they are in contact, very close to one another, and concentrated in the periphery of the metal particles, at the metal–support interface, as proposed by several authors (9, 11, 12), or (b) these sites are separated, but important and rapid surface diffusion of species between the metal and the support enables a major part of the active centers of the oxidic support and the metal to be active in the reaction. This latter option is supported by results obtained by Nakamura *et al.* (6), in which the activity of a Rh/SiO_2 catalyst was greatly promoted by mixing it physically with metal oxides, such as γ-Al_2O_3, TiO_2, or MgO.

Aiming to discriminate between these possibilities and further determine the importance of the interfacial sites, a series of bimetallic catalysts supported on alumina has been synthesized. The elements composing the metallic phase are rhodium, one of the most active metals for methane activation, and copper, almost inactive for this process, at least at moderate temperatures (15). This series of bimetallic catalysts has been tested in reaction with CH_4 and with $CH_4 + CO_2$. Catalytic activity measurements, hydrogenation of the carbonaceous deposits resulting from methane decomposition, and *in situ* spectroscopic examination of the adsorbed species and of the state of the metallic phase have made possible to evaluate the role of the interfacial sites in these reactions. Comparison of these results with those obtained for a Rh/SiO_2 catalyst in reaction has led us to draw important conclusions about the surface migration

0021-9517/00 $35.00

phenomena on these systems and their importance in the catalysis of methane activation and its reforming with carbon dioxide.

EXPERIMENTAL

A series of four bimetallic catalysts was prepared by coimpregnation of γ-Al_2O_3 (Puralox Condea, $S_{\mathrm{BET}} = 175$ m^2 g^{-1}) with aqueous solutions of $RhCl_3 \cdot xH_2O$ ($x = 1$, 3) (Aldrich Chemie) and $Cu(NO_3)_2 \cdot 3H_2O$ (Alfa) according to the incipient wetness impregnation technique. The concentration of the precursors was calculated to obtain different Rh : Cu ratios in the range between 0.05 and 0.43 with a 5 wt% total metal loading. As a reference for each of the components of these catalysts, two monometallic samples, Rh/Al_2O_3 (ca. 1 wt% rhodium loading) and Cu/Al_2O_3 (ca. 5 wt% copper loading), were prepared. A silica specimen (Aerosil 200, Degussa, $S_{\mathrm{BET}} = 180$ m^2 g^{-1}) was also impregnated with an aqueous solution of the same rhodium precursor salt, in order to obtain a ca. 1 wt% Rh/SiO_2 catalyst. After impregnation, the resulting powders were dried overnight and calcined for 3 h in air at 773 K. Before use, the samples were reduced *in situ* in pure H_2 (20 cm^3 min^{-1} (STP) for 2 h at 673 K. The prepared catalysts and their main characteristics are listed in Table 1.

Metal contents were analyzed by atomic absorption. Metal dispersion of rhodium was determined by H_2 chemisorption at room temperature in a volumetric system and assuming an adsorption stoichiometry of 1H : 1Rh. Samples were first reduced in hydrogen flow at 823 K for 2 h.

For catalytic testing, the samples were placed in a tubular quartz U-shaped reactor. The temperature was controlled by means of a K-type thermocouple close to the reactor wall. For methane interaction tests, ca. 0.25 g of catalyst was used. Temperature-programmed surface reaction (TPSR) experiments with methane were carried on pre-reduced and cleaned samples by heating them from 298 to 873 K at a rate of 10 K min^{-1}. The reactor was fed with a diluted mixture of 7% (vol) CH_4 in He (102 cm^3 min^{-1} STP) adjusted by mass flow controllers (Brooks, model 5850 TR) and operating at a pressure of 150 kPa. The reaction system was connected to a gas chromatograph (Varian 3400) in series with a quadrupole mass spectrometer (Balzers QMG 421-C). A leak valve permitted control of the inlet of effluent into the mass spectrometer UHV chamber. The different m/z values registered during the experiment ($H_2 = 2$; $He = 4$; $CH_4 = 14$, 16; $C_2H_2 = 25$; $C_2H_4 = 27$; $CO = 28$; $C_2H_6 = 30$; $CO_2 = 44$) were collected on an interfaced computer.

TABLE 1

Main Characteristics and Chemisorption Data of the Catalysts

Sample	Metal loading		Rh–Cu	H_2 uptake	
	% Rh	% Cu	(at.%)	(μmol/g)	H/Rh
Rh/Al_2O_3	1.25	—	100–0	22.1	0.36
Cu/Al_2O_3	—	4.84	0–100	—	—
$0.05RhCu/Al_2O_3$	0.45	4.6	5–95	11.5	0.53
$0.14RhCu/Al_2O_3$	0.95	4.2	12–88	16.8	0.36
$0.23RhCu/Al_2O_3$	1.40	3.8	19–91	24.4	0.36
$0.43RhCu/Al_2O_3$	2.05	3.0	30–70	27.0	0.27
Rh/SiO_2	1.21	—	100	34.5	0.59

The activity for the decomposition of methane was also tested with the same reaction mixture under isothermal conditions at 623 K for 3 h. In order to analyze the total amount, the kind, and the reactivity of the species generated during that period, temperature-programmed hydrogenation (TPH) of these carbon deposits was performed. After the reaction with methane, the reactor was cooled and residual CH_4 was cleaned from it in a flow of He. Then, it was fed with a mixture of 14% (vol) H_2 in He (35 cm^{-3} min^{-1} (STP)) while heating from 298 to 773 K at a rate of 7 K min^{-1}. The outlet mixture was analyzed by gas chromatography.

For each activity test of reforming, the amount of catalyst used (10–50 mg) was adjusted to maintain CH_4 and CO_2 conversions far from those predicted by the thermodynamic equilibrium. After reduction, the samples were heated in helium to the reaction temperature (823 K). A reaction mixture of $CH_4 + CO_2 + He$ in a 10 : 10 : 80 proportion and regulated by mass flow controllers was adjusted to give a flow rate of 100 cm^3 min^{-1} (STP). Reactants and products were analyzed by online gas chromatography (Varian 3400) using a thermal conductivity detector and an automatic sampling valve. Chromosorb 102 and Porapak Q columns, connected in series, were used to achieve separation of H_2, CH_4, CO, and CO_2.

In situ spectroscopic examination of the samples was performed with a Perkin-Elmer 1750 spectrometer equipped with a diffuse reflectance accessory and a liquid nitrogen-cooled MCT detector. After reduction, the sample was heated to the reaction temperature (723 or 823 K) and a spectrum of the clean sample obtained. The reaction was carried out by admitting a flow of 100 cm^3 min^{-1} (STP) of $CO_2 + N_2$ in a 10 : 90 proportion. After reaching a steady state the feed was substituted by a flow of $CH_4 + CO_2 + N_2$ in a 10 : 10 : 80 proportion. After 15 min in reaction, the inlet mixture composition was changed by removing one (CH_4 or CO_2) or both of the reactants, and changes in the spectrum induced at each of these stages were analyzed. Finally, DRIFT spectra of the adsorbed species were obtained by subtraction of the initial spectrum, registered under inert gas flow, from those obtained under $CH_4 + CO_2 + N_2$, $CO_2 + N_2$, and $CH_4 + N_2$ mixtures and the same temperature. All spectra measured in reflectance were subsequently converted via Kubelka–Munk transformation.

X-ray absorption near edge spectroscopy (XANES) experiments were performed at the Rh and Cu *K*-edges on beam line ID-24 at ESRF synchrotron, Grenoble, France. All samples, catalysts and pure reference compounds, were measured in an energy dispersive transmission mode with simultaneous calibration of the energy scale with a rhodium or copper foil. A bent perfect Si crystal in a Bragg configuration was used as a dispersive monochromator. Self-supporting wafers of approximately equal absorbance were placed in a controlled atmosphere cell and submitted to the required temperature. The wafers were firstly reduced in a diluted mixture of 10% H_2 in He by heating at 3 K/min from 298 to 673 K, maintaining this last temperature for 15 min. After the reduction pretreatment, the sample was submitted to reaction conditions at 823 K for 15 min under a $CH_4 + CO_2 +$ He mixture in a 10 : 10 : 80 proportion. Then, CH_4 was removed from the inlet flow and the sample was maintained under this environment for another 15 min. Finally, the $CO_2 +$ He mixture was replaced by a $CH_4 +$ He flow. A XANES spectrum was recorded every 5 min for these three periods after the inlet mixture composition was changed.

X-ray photoelectron analysis was performed over reduced samples used in reaction with CH_4 and CO_2 at 823 K for 3 h, aiming to analyze the surface oxidation state of the metal. To avoid oxidation by contact with air, these latter specimens were recovered from the reactor and immersed in isooctane to transport them to the analysis chamber. A multitechnique instrument for surface analysis ESCA/XPS, AES, from Fisons Instruments, was used. The excitation source was the Mg$K\alpha$ line ($h\nu = 1253.6$ eV). The pressure in the analysis chamber was kept below 10^{-9} Torr during acquisition. Binding energies were referenced to the Al 2p line at 74.7 eV.

RESULTS

Interaction with Methane

The interaction of methane with the different catalysts was studied by TPSR experiments. Figure 1 displays, in comparison with the monometallic catalysts of Rh/Al_2O_3 and Cu/Al_2O_3, the amount of hydrogen produced by CH_4 decomposition over each of the samples as a function of the reaction temperature. The hydrogen evolution profiles reflect great differences in activity for methane activation between rhodium and copper. Bimetallic systems showed initially very similar levels of activity for the dehydrogenation process of CH_4 and slightly lower than that of monometallic rhodium catalyst, despite their distinct loading of active metal (Rh). The difference in performance among the bimetallic catalysts became greater with increasing temperature. Under high-temperature conditions (above 723 K), the catalysts with higher Rh : Cu ratios achieved an activity level close to that shown by the monometallic Rh/Al_2O_3 sample, while $0.05RhCu/Al_2O_3$ and $0.14RhCu/Al_2O_3$ have a significantly lower dehydrogenation ability.

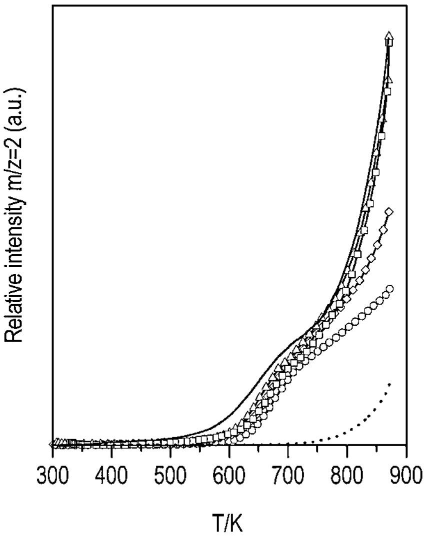

FIG. 1. Hydrogen production on the $RhCu/Al_2O_3$ catalysts during the TPSR experiments. The monometallic Rh/Al_2O_3 and Cu/Al_2O_3 references are included for comparison. Reactant mixture: CH_4 (7% vol) in He. Gas flow rate: 6.1 1 h^{-1}. Rate of temperature increase: 10 K/min. Symbols: (□) $0.43\ RhCu/Al_2O_3$, (△) $0.23\ RhCu/Al_2O_3$, (◇) $0.14\ RhCu/Al_2O_3$, (○) $0.05\ RhCu/Al_2O_3$, (—) Rh/Al_2O_3, and (···) Cu/Al_2O_3.

As previously shown for several group VIII metals (5), hydrogen evolution resulting from the interaction of methane with supported catalysts was observed to be followed by the formation and release of carbon monoxide as a result of the consumption of hydroxyl groups of the support. As an example, the level of conversion obtained for one of the catalysts ($0.43RhCu/Al_2O_3$), in addition to the methane consumption, the hydrogen and carbon monoxide production, and the cumulative amount of carbon retained on the catalyst per surface rhodium site, are given in Table 2. A simple mass balance calculated on the basis of CH_4 consumed and H_2 produced along with the experiment indicates that the dehydrogenation of methane is almost complete at temperatures above 673 K. The amount of hydrogen produced duplicates the methane consumption with a difference lower than 5%, indicating that each molecule of CH_4 is completely dehydrogenated, resulting in two H_2 molecules. The amount of carbon deposited at high temperatures exceeds greatly the number of surface rhodium sites, as indicated by the $C/M_{\mathrm{Rh\ surface}}$ ratio in Table 2. Taking into account that this catalyst maintains a high activity level at high temperatures, a process of carbon migration from the metal to the support that leaves the active centers free has to be considered. Furthermore, transmission electron microscopy observations of the spent samples revealed the absence of formation of carbon deposits with crystalline structure.

The reactivity of the different samples with methane was also tested under isothermal conditions at 623 K for 3 h. Methane conversion was lower than 2% in all cases, and hydrogen production could not be quantified under these conditions. However, the level of CO produced was

TABLE 2

Temperature-Programmed Surface Reaction with Diluted Methane on the 0.43RhCu/Al_2O_3 Sample

T/K	Conv. (%)	CH_4 consumption (μmol g^{-1} s^{-1})	H_2 production (μmol g^{-1} s^{-1})	CO production (μmol g^{-1} s^{-1})	C/$M_{Rh\ surface}$[a]
300	0.5	0.22	0.0	0.0	0.0
333	0.6	0.23	0.0	0.0	0.0
388	0.6	0.21	0.0	0.0	0.0
445	0.7	0.25	0.0	0.0	0.0
499	0.9	0.31	0.0	0.0	0.0
552	1.3	0.46	0.58	0.0	1.64
604	2.1	0.76	1.59	0.33	5.85
658	3.3	1.18	2.26	0.61	11.54
715	4.5	1.59	3.19	0.87	19.13
769	8.7	3.07	6.27	0.95	35.94
822	15.7	5.57	11.22	0.97	74.65
873	22.3	7.94	15.96	0.81	139.10

Note. Mixture, CH_4 (7% vol) in He; flow rate, 102 cm^3/min; heating rate, 10 K/min.

[a] Atomic ratio between the cumulative amount of carbon retained on the catalyst and the surface rhodium sites. The total amount of carbon has been calculated on the base of the methane consumed to produce two hydrogen molecules and the carbon monoxide released ($X_c = 1/2\ X_{H_2} - X_{CO}$).

accurately followed. The amount of CO released, shown in Fig. 2, is very similar for all rhodium bimetallic samples. This fact seems to indicate that its rate of formation does depends not on the number of surface rhodium sites but on the equilibrium between the rate of diffusion of hydroxyl groups from the alumina to the metal and/or the rate of migration of the carbonaceous adspecies generated on rhodium sites toward the support. These two processes of migration leave rhodium sites free for the adsorption and activation of other methane molecules, allowing the whole reaction to reach a stationary state.

In order to obtain information regarding the type of carbonaceous adspecies generated during the previous isothermal step of interaction of the catalysts with methane, their reactivity toward hydrogen was studied. The amount of carbon retained was estimated from the carbonaceous deposits that could be hydrogenated in the temperature range from 298 to 773 K. During the hydrogenation process no hydrocarbon other than methane was detected for all catalysts. The CH_4 evolution profiles obtained during the TPH for all the bimetallic samples are displayed in Fig. 3. Three types of carbon could be distinguished: a first type of species of

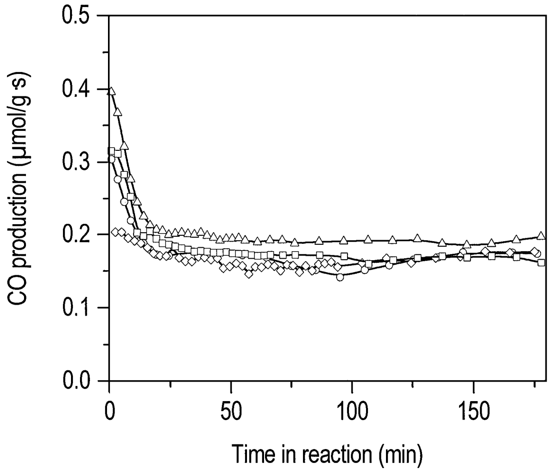

FIG. 2. Carbon monoxide production on the RhCu/Al_2O_3 catalysts during the interaction with diluted methane at 623 K. Reactant mixture: CH_4 (7% vol) in He. Gas flow rate: 6.1 1 h^{-1}. Symbols: (□) 0.43 RhCu/Al_2O_3, (△) 0.23 RhCu/Al_2O_3, (◇) 0.14 RhCu/Al_2O_3, and (○) 0.05 RhCu/Al_2O_3.

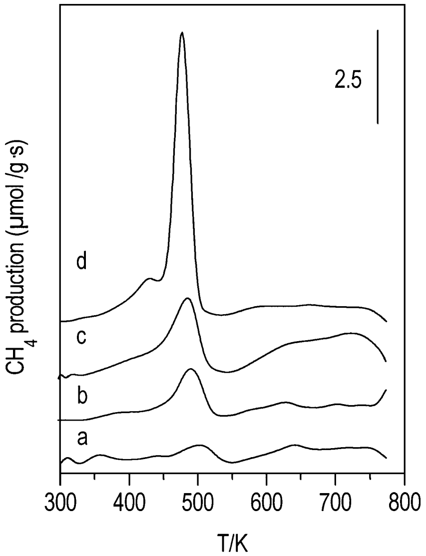

FIG. 3. Methane production obtained by temperature-programmed hydrogenation of the carbonaceous deposits formed from methane decomposition on the RhCu/Al_2O_3 catalysts at 623 K. Reactant mixture: CH_4 (7% vol) in He. Gas flow rate: 6.1 1 h^{-1}. Rate of temperature increase: 7 K/min. (a) 0.05 RhCu/Al_2O_3, (b) 0.14 RhCu/Al_2O_3, (c) 0.23 RhCu/Al_2O_3, and (d) 0.43 RhCu/Al_2O_3.

TABLE 3

Total Amount of Carbon Species Hydrogenated at Temperatures up to 773 K from the Catalysts Previously Submitted to a Flow of Diluted Methane at 623 K for 3 h

Catalyst	$C_{hydrogenated}$ (μmol g^{-1})	$C_{500\ K}$ (μmol g^{-1})	$Rh/C_{500\ K}$
$0.05RhCu/Al_2O_3$	37.0	14.95	2.9
$0.14RhCu/Al_2O_3$	50.92	26.19	3.5
$0.23RhCu/Al_2O_3$	114.10	49.87	2.8
$0.43RhCu/Al_2O_3$	89.72	65.19	3.1
Rh/Al_2O_3	99.55	34.62	3.5

high reactivity, hydrogenatable at temperatures lower than 373 K; a second type of carbon hydrogenatable between 373 and 523 K, with two hydrogenation maxima at ca. 425 and 500 K; and, finally, a third type which can be hydrogenated in a wide range of temperatures above 523 K.

The amount of species showing well-defined hydrogenation maxima around 500 K was observed to increase with the rhodium loading in the catalyst. A displacement in the hydrogenation temperature of these species toward lower values, close to that observed for the Rh/Al_2O_3 catalyst (ca. 460 K), was also obtained by increasing the Rh : Cu ratio. Table 3 summarizes the total amount of carbon retained on the various samples and the part corresponding to the species hydrogenated at temperatures around 500 K. This latter type of carbon has been shown to keep a well-defined stoichiometry with respect to the whole rhodium loading in the catalyst, as indicated by the $Rh/C_{500\ K}$ ratio in Table 3.

Reaction with CH_4 and CO_2

Catalytic Activity Tests. The four alumina-supported rhodium–copper samples were tested in reaction with CH_4 and CO_2 at 823 K in comparison with the monometallic Rh/Al_2O_3 and Cu/Al_2O_3 catalysts. A Rh/SiO_2 sample was also tested to evaluate the influence of the alumina on the rhodium catalytic performance. Table 4 compiles initial values, obtained after 10 min of reaction, for conversion of reactants, specific activity for methane transformation (converted methane amount per gram of rhodium and per second), turnover frequency (converted methane per surface rhodium site and per second), and degree of stability after 3 h of reaction.

TABLE 4

Catalytic Properties of the Rhodium–Copper Bimetallic Catalysts in Reaction with $CH_4 + CO_2$ at 823 K

Catalyst	Conv. (%) CH_4	Conv. (%) CO_2	r_{CH_4} (mmol g_{Rh}^{-1} s^{-1})	TOF_{CH_4} (s^{-1})	$r_{180\ min}/r_{10\ min}$
$0.05RhCu/Al_2O_3$	18	19	16.84	3.3	0.88
$0.14RhCu/Al_2O_3$	20	22	8.66	2.4	0.92
$0.23RhCu/Al_2O_3$	27	28	7.94	2.3	0.83
$0.43RhCu/Al_2O_3$	28	32	7.94	2.2	0.83
Rh/Al_2O_3	32	37	10.72	3.0	0.99
Cu/Al_2O_3	0	0	—	—	—
Rh/SiO_2	16	21	1.41	0.2	0.12

Note. Reactant mixture, $CH_4 : CO_2 : He$ (10 : 10 : 80); Flow rate, 100 cm^3/min.

A first analysis of the data obtained for the monometallic rhodium samples, Rh/SiO_2 and Rh/Al_2O_3, reveals prominent differences between them concerning not only their catalytic activity level but also their stability under the reaction conditions. In terms of turnover frequency, the Rh/Al_2O_3 sample exhibits an enhanced performance, about 1 order of magnitude higher of that of Rh/SiO_2. Even considering that the metal–support interaction might affect the energy of the atomic hydrogen adsorption on rhodium and, therefore, modify H : Rh ratios (16), a comparison of the values of catalytic activity calculated on the basis of the whole rhodium loading confirms the previous statement about the influence of the support on the catalytic activity. A contrasting behavior was also found with regard to the stability under reaction conditions. While Rh/SiO_2 lost about 88% of its initial activity after 3 h of reaction with CH_4 and CO_2, the conversion for Rh/Al_2O_3 remained unmodified with time.

Bimetallic catalysts behaved in a similar way to the monometallic reference of Rh/Al_2O_3. However, some particularities can be noticed. Turnover numbers do not reflect significant differences in activity per surface rhodium site and all of them are in the same range of the value obtained for the monometallic rhodium reference. On the other hand, copper is completely inactive for the reaction due to its inability to dehydrogenate methane. By considering that, in addition to the strong interaction of rhodium with the alumina support, the presence of copper might also modify the hydrogen adsorption properties of rhodium (17), comparison of the catalytic activity per gram of active metal (Rh) in each of the $RhCu/Al_2O_3$ samples has been performed. These values indicate that the addition of copper to catalysts slightly changes the catalytic activity. Nevertheless, the degree of stability of the bimetallic samples was more significantly affected by copper as compared with the excellent maintenance of the conversion on the Rh/Al_2O_3 catalyst. Each bimetallic sample experienced a decay of its initial activity in the range between 8 and 17 % after 3 h of reaction.

In situ DRIFT analysis. *In situ* infrared spectroscopic examination of the samples was carried out with the objective of identifying the adsorbed intermediate species present on the catalyst surface under the reaction conditions and trying to elucidate the causes that lead to such a different behavior of the catalysts depending on their support and on the composition of their metallic interfacial sites. Changes in the DRIFT spectra were monitored in response to changes in the gas phase composition.

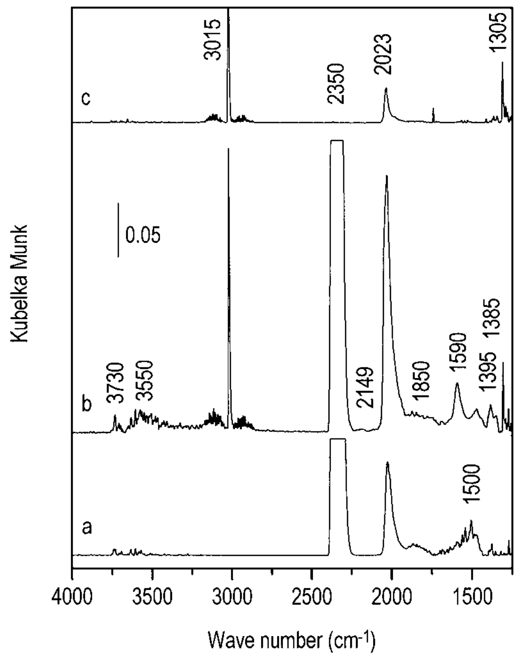

FIG. 4. DRIFT spectra obtained for the Rh/Al_2O_3 catalyst at 723 K: (a) under $CO_2 + N_2$ (10 : 90) mixture (100 cm^3/min), (b) under reforming conditions $CH_4 + CO_2 + N_2$ (10 : 10 : 80) (100 cm^3/min), and (c) under $CH_4 + N_2$ (10 : 90) mixture (100 cm^3/min).

Rh/Al_2O_3. Apart from the gas phase contributions (CO_2 centered at ca. 2350 cm^{-1}, CH_4 at ca. 3015 and 1305 cm^{-1}, and CO at ca. 2149 cm^{-1}), some other features corresponding to adsorbed intermediates could be identified in the DRIFT spectra collected for the Rh/Al_2O_3 catalyst at 723 K, which are shown in Fig. 4.

Under diluted carbon dioxide, a small coverage of the rhodium surface sites was observed as result of the formation of linearly and bridge bound carbon monoxide on metallic rhodium (bands at ca. 2023 and 1850 cm^{-1}, respectively). At 1500 cm^{-1} a broad feature, most likely characteristic of carbonate type species adsorbed on the alumina support at high temperatures (18, 19), became apparent. When methane and carbon dioxide were introduced simultaneously in the feeding, bands corresponding to the formation of rhodium carbonyl increased in their intensity. On the contrary, the feature at 1500 cm^{-1} was almost depleted while three bands at ca. 1590, 1395, and 1385 cm^{-1} became apparent. These latter bands can be assigned to surface-adsorbed formate species formed on the alumina support (20). The appearance of these bands is accompanied by an increase of the absorption bands in the region between 3500 and 3800 cm^{-1}, corresponding to the O–H stretching frequency of the hydroxyl groups of the alumina. By removing carbon dioxide from the reactant mixture, only carbonyl bands remained in the spectrum. At a higher temperature (823 K), the same trend as that at 723 K was observed, though the coverage of the different adspecies decreased significantly.

Bands corresponding to formate adsorbed species, HCO_2^- have been frequently related to the adsorption of CO on the alumina surface (21). Thus, they have been considered by different authors as byproducts of the reaction (22–24). Aiming to shed light on these questions, DRIFT spectra were collected for the carbon monoxide adsorption on the Rh/Al_2O_3 catalyst under a flow of diluted CO (5% vol CO in N_2) at increasing temperatures. Figure 5 displays spectra taken at room temperature and at 523 K under flowing $CO + N_2$ in comparison with the one obtained under reaction conditions with CH_4 and CO_2 at 723 K.

Adsorption of CO at room temperature gave rise to an intense band at ca. 2057 cm^{-1} and another broad feature of lower intensity centered around 1850 cm^{-1}, assigned to linearly and bridge adsorbed CO on metallic rhodium, respectively. At ca. 1620 cm^{-1} a band due to water molecularly adsorbed on the support became apparent and at 1590, 1395, and 1385 cm^{-1} bands due to adsorbed formate species. The increase of the temperature to 523 K caused the intensity of the CO adsorption peaks to decrease by 36% and the peak maximum of linear adsorbed CO to be displaced to lower wavenumbers (ca. 2037 cm^{-1}). At this temperature water and formate absorption bands became almost completely depleted, indicating the instability of these species at high temperatures. Under reaction conditions with methane and carbon dioxide at 723 K, the band due to linearly bound carbon monoxide on rhodium was slightly displaced to lower frequency (ca. 2029 cm^{-1}) and its intensity decreased by about 29% as compared with the intensity of the CO adsorption band at room temperature.

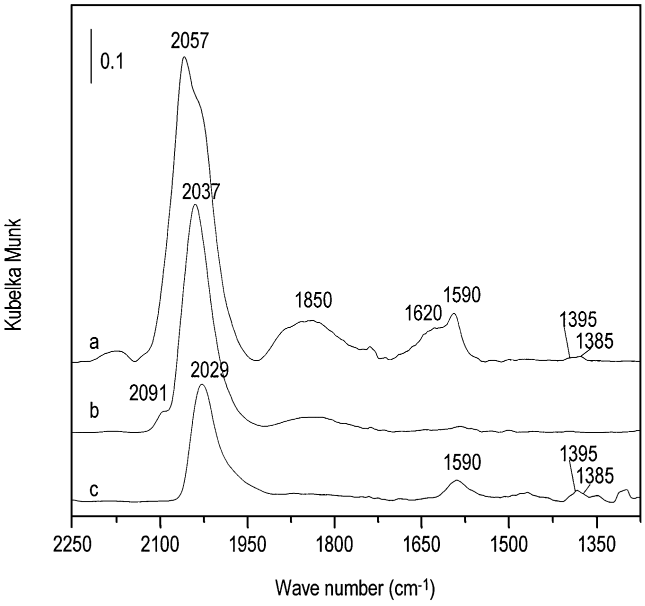

FIG. 5. DRIFT spectra obtained for the Rh/Al_2O_3 catalyst: (a) under a flow of CO (5% vol) in N_2 at 298 K, (b) under a flow of CO (5% vol) in N_2 at 523 K, and (c) under the reaction mixture $CH_4 + CO_2 + N_2$ (10 : 10 : 80) at 723 K.

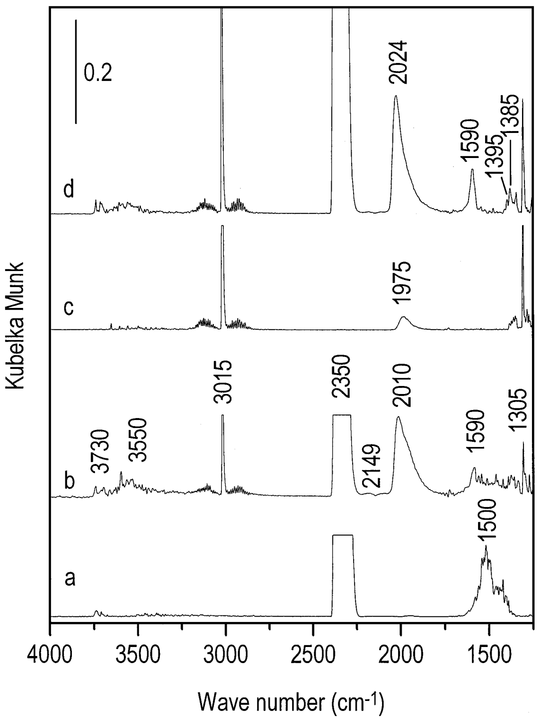

FIG. 6. DRIFT spectra obtained for the 0.14 RhCu/Al_2O_3 catalyst at 823 K: (a) under $CO_2 + N_2$ (10 : 90) mixture (100 cm^3/min), (b) under reforming conditions $CH_4 + CO_2 + N_2$ (10 : 10 : 80) (100 cm^3/min), and (c) under $CH_4 + N_2$ (10 : 90) mixture (100 cm^3/min). (d) DRIFT spectrum obtained for the 0.14 RhCu/Al_2O_3 catalyst at 723 K under reforming conditions $CH_4 + CO_2 + N_2$ (10 : 10 : 80) (100 cm^3/min).

Features due to adsorbed formate species became apparent with intensity even higher than that obtained under flowing carbon monoxide at room temperature. The appearance of these bands indicates the formation of these species under specific reaction conditions.

0.14RhCu/Al_2O_3. One of the bimetallic samples, 0.14RhCu/Al_2O_3, was analyzed by DRIFTS for comparison with the Rh/Al_2O_3 reference. Figure 6 shows the spectra collected under $CO_2 + N_2$, $CH_4 + CO_2 + N_2$, and $CH_4 + N_2$ flows at 823 K and under $CH_4 + CO_2 + N_2$ at 723 K. Tendencies similar to those observed on the monometallic alumina-supported catalyst are observed.

Apart from the characteristic bands from the gas phase, a broad feature around ca. 1500 cm^{-1} due to carbonate type species adsorbed on the alumina was observed under flowing carbon dioxide. When CH_4 was introduced together with CO_2 in the inlet feed, this latter band was reduced while characteristic bands of formate species developed. Simultaneously, an increase in the absorption intensity of the stretching modes of alumina surface hydroxyls (ca. 3550 cm^{-1}) was observed. Carbon monoxide absorption bands were obtained only for linearly adsorbed CO on Rh^0 (2010 cm^{-1}). Under diluted methane all the previously described features disappeared, with the exception of the linearly bound CO on metallic rhodium (band at ca. 1975 cm^{-1}) that showed to be constant with time. At a lower reaction temperature (723 K) under reaction conditions with $CH_4 + CO_2 + N_2$ the relative intensity of bands stemming from formate species was increased.

Rh/SiO_2. The substitution of an inert flow of N_2 by $CO_2 + N_2$ (10 : 90) at 723 K gave rise to the appearance of a band at ca. 2036 cm^{-1} whose intensity was observed to decrease with time. This band has been ascribed to the C–O stretching frequency of carbon monoxide linearly bound to rhodium particles (25, 26). The admission of the reactant mixture, $CH_4 + CO_2 + N_2$ (10 : 10 : 80), led to the increase of this latter feature whose intensity remained stable for the 15 min of reaction. After this time had elapsed, carbon dioxide was removed from the reaction mixture. In contrast to alumina-supported samples, under $CH_4 + N_2$ (10 : 90) this carbonyl band decreased progressively until complete disappearance. At 823 K no adsorbed species were detected due to the low coverage of the catalyst surface.

XANES study. The catalysts were also studied *in situ* by XANES at 823 K under $CH_4 + CO_2 + He$, $CO_2 + He$, and $CH_4 + He$ flows.

Figure 7 shows XANES spectra obtained for two of the bimetallic RhCu systems (0.14 RhCu/Al_2O_3 and 0.43RhCu/Al_2O_3) and the copper monometallic reference

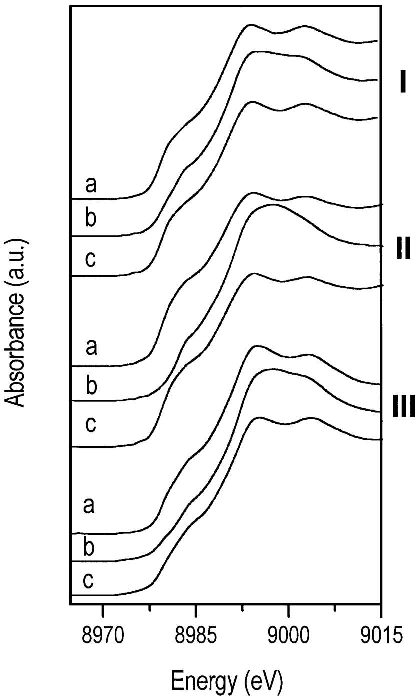

FIG. 7. XANES profiles obtained in situ at 823 K in the Cu K-edge for the 0.14 RhCu/Al_2O_3 (**I**) and 0.43 RhCu/Al_2O_3 (**II**) bimetallic samples and the copper monometallic reference (Cu/Al_2O_3) (**III**) after 15 min: (a) under reforming conditions $CH_4 + CO_2 + He$ (10 : 10 : 80), (b) under $CO_2 + He$ (10 : 90) mixture, and (c) under $CH_4 + He$ (10 : 90) mixture.

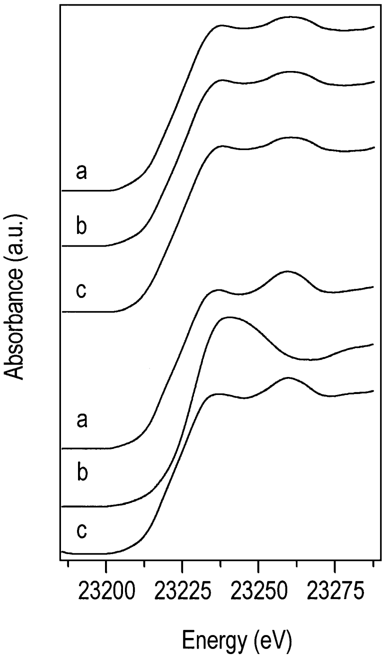

FIG. 8. XANES profiles obtained *in situ* at 823 K for Rh/Al_2O_3 (**I**) and Rh/SiO_2 (**II**) after 15 min: (a) under reforming conditions $CH_4 + CO_2 + He$ (10 : 10 : 80), (b) under $CO_2 + He$ (10 : 90) mixture, and (c) under $CH_4 + He$ (10 : 90) mixture.

in the K-edge Cu. A qualitative analysis of these profiles indicates that for all these samples copper remains in its metallic state after reduction under $CH_4 + CO_2$ reaction conditions. Under carbon dioxide atmosphere, the copper (Cu^0) in Cu/Al_2O_3 became slowly oxidized with time; the spectrum obtained after 15 min (Fig. 7, IIIb) contains a contribution from CuO in addition to the initial phase of Cu^0. When the $CH_4 + CO_2 + He$ feed was substituted by diluted carbon dioxide, a certain contribution of a CuO phase was also observed in the XANES spectrum for copper on both bimetallic catalysts. This contribution was observed to be higher in the lower copper loading catalyst, which suffered an almost complete oxidation. Upon the introduction of the $CH_4 + He$ (10 : 90) mixture in the reactor these CuO phases were again reduced. No alteration was detected in the metallic state for the rhodium phase on alumina-supported catalysts. The phase of rhodium on the bimetallic specimens remained unmodified as Rh^0 under diluted carbon dioxide, diluted methane, or methane and carbon dioxide mixture, showing a higher resistance to oxidation by CO_2 than copper.

The same trend was observed for rhodium in the alumina monometallic reference. Figure 8 displays the XANES spectra obtained for the Rh/Al_2O_3 catalyst, which remained unmodified even under carbon dioxide atmosphere. The presence of the alumina support seems to influence the oxidation rate of the metal, given that a different behavior of Rh was observed on the Rh/SiO_2 system (Fig. 8). With the reaction mixture, the XANES spectrum revealed that rhodium remained in the metallic state. When the reactant mixture was substituted by diluted carbon dioxide, rhodium was completely oxidized to Rh^{3+} in a few minutes, but the metallic state was again restored when diluted methane was introduced in the reactor, indicating that Rh_2O_3 is also able to activate methane.

XPS results. By considering that the XANES spectroscopic analysis provides global information about the major part of the photoexcited centers in the samples, i.e., surface and bulk atoms, the 0.14 $RhCu/Al_2O_3$, and $0.43RhCu/Al_2O_3$ were analyzed by XPS after being submitted to a $CH_4 + CO_2$ mixture at 823 K for 3 h in order to detect the presence of oxidized phases at the surface. The results obtained for these bimetallic catalysts after reaction are compiled in Table 5. Data obtained for the 0.14 $RhCu/Al_2O_3$ sample after reduction are also given for comparison.

The 0.43 $RhCu/Al_2O_3$ catalyst showed the presence of the peaks characteristic of the 3d levels of Rh^0 with binding energies centered at 307.9 and 312.2 eV, respectively, for Rh 3d5/2 and Rh 3d3/2. The 0.14 $RhCu/Al_2O_3$ sample was analyzed after reduction at 673 K and after being tested in reaction. In both cases, the presence of Rh^0 was again found on the surface, with binding energies of 311.8 and 307.5 eV. Analysis of the copper surface in both bimetallic samples used in reaction and in the 0.14 $RhCu/Al_2O_3$ after reduction at 673 K showed the Cu 2p1/2 and Cu 2p3/2 peaks at binding energies of 953.2 and 933.0 eV corresponding to Cu^0, in agreement with the XANES results.

TABLE 5

Data Obtained from XPS Analysis on the $0.14RhCu/Al_2O_3$ and the $0.43RhCu/Al_2O_3$ Samples

	Binding energy (eV)			Binding energy (eV)		
Sample[a]	Rh 3d3/2	Rh 3d5/2	Assignment	Cu 2p1/2	Cu 2p3/2	Assignment
(I) $0.14RhCu/Al_2O_3$	311.8	307.4	Rh^0	952.6	933.1	Cu^0
(I) $0.43RhCu/Al_2O_3$	312.2	307.9	Rh^0	953.2	933.0	Cu^0
(II) $0.14RhCu/Al_2O_3$	311.8	307.5	Rh^0	952.5	933.0	Cu^0

[a] (I) After being tested in reaction with $CH_4 + CO_2$ at 823 K for 3 h. (II) After reduction at 673 K for 2 h.

DISCUSSION

Activation of Methane

The hydrogen evolution process from methane decomposition reveals great differences in activity for methane activation between rhodium and copper, as recently indicated by Liao and Zhang (15). In a theoretical study regarding the dissociation of methane on several transition metals they have shown that there is a direct correlation between the values calculated for the enthalpy of total dissociation of methane and the experimental activity measured on them. Among several group VIII metals, rhodium and nickel have been shown to be the only ones on which this process is slightly exothermic, in contrast with metals such as ruthenium, iridium, platinum, or palladium, for which methane dissociation is endothermic. For group IB metals (Cu, Ag, and Au), much higher reaction enthalpies were obtained, indicating an almost complete inactivity for methane activation. The results obtained over the monometallic Rh/Al_2O_3 and Cu/Al_2O_3 catalysts are in agreement with these earlier reports.

A comparison of the reactivity presented by the bimetallic $RhCu/Al_2O_3$ samples and the Rh/Al_2O_3 and Cu/Al_2O_3 references (Fig. 1) shows an intermediate behavior that indicates in all cases a certain interaction between both metallic components. Even in the case of the 0.43 $RhCu/Al_2O_3$ catalyst with higher rhodium loading and a higher number of exposed Rh atoms according to the chemisorption experiment, a decrease in activity was found as a result of copper addition. A certain delay in the temperature at which the reaction begins (∼550 K) on Rh/Al_2O_3 could be observed for the bimetallic samples, particularly on those with higher copper content.

The methane activation process is favored in the presence of a certain amount of oxygen (15, 17, 28), which is usually present on the support surface as hydroxyl groups (5, 13). The reaction of these hydroxyl groups with the carbonaceous adspecies formed from methane decomposition results in a parallel process of carbon monoxide evolution, as shown for the 0.43 $RhCu/Al_2O_3$ sample during the TPSR experiment (Table 2). By taking into account the surface hydroxyl concentration on alumina previously submitted to a dehydration treatment between 720 and 870 K (about 5–12 OH nm^{-2}) and the high surface area of the alumina used (175 $m^2\ g^{-1}$), an average value of 8 OH nm^{-2} would correspond to an estimated amount of surface hydroxyls of 2.3 mmol g^{-1}, which would account for 4 wt% of the support. For the particular case of the 0.43 $RhCu/Al_2O_3$ catalyst the total amount of CO evolved in the TPSR experiment is 1.33 mmol g^{-1} of catalyst, which would suppose a consumption of about 57% of the hydroxyl groups present on the support surface.

On the other hand, even though a part of the surface carbonaceous adsorbed species is removed from the catalyst by oxidation with OH groups in the form of CO, methane has been shown to be activated and accumulated on the catalysts in much higher amounts than those corresponding to the number of exposed active centers (Table 2). Thus, another important step to take into account in this process is the surface migration of carbonaceous adspecies from the active sites (Rh) toward the inactive zones of the catalyst, i.e., the support (4, 29) or the copper phase (30, 31). Both processes of migration of species will finally determine the availability of active rhodium sites for methane activation. On this basis, it can be considered that the active metal (Rh) acts simply as an initiator for the hydrogenation reaction, but the activity level measured on the catalyst will depend on the ratio between the rates of diffusion of hydroxyl groups from the alumina support to the rhodium and of carbonaceous adspecies from the rhodium to the inactive zones (the alumina or the copper surface).

From this standpoint, the activity of the catalysts (Figure 1) will be determined by the degree of hydroxylation of the support, which can be considered the same for all samples, and also by the rate of diffusion of species (OH and CH_x) between the active phase and the support. In the case of the 0.23 $RhCu/Al_2O_3$ and 0.43 $RhCu/Al_2O_3$ samples, which do not display alloying between metal components, particle size or most likely the presence of nonalloyed copper in the rhodium particle surface (17) diminishes the interface of contact between the rhodium surface centers and the alumina and therefore decreases the surface diffusion processes of species between them. At high temperatures, however, the differences are progressively reduced. On the other hand, on 0.05 $RhCu/Al_2O_3$ and 0.14 $RhCu/Al_2O_3$ catalysts, which contain alloyed phases and for which the surface is enriched in copper (17), the dehydrogenating ability was found to decrease to a great extent.

During the isothermal interaction of methane with the catalysts at 623 K the removal of carbonaceous adspecies by reaction with the alumina hydroxyls was found to occur for all the catalysts to the same extent (Figure 2). The analysis of the reactivity of the carbonaceous deposits generated by this isothermal step on the bimetallic catalysts revealed the presence of three types of species, which fit perfectly in the classification of Koerts *et al.* proposed for the carbon deposits formed from methane decomposition on several silica-supported metals (32).

The most reactive species, C_α or carbidic carbon, hydrogenatable below 373 K, was found in low proportion on the alumina-supported catalysts. In a previous study concerning the methane interaction with supported catalysts, it was shown that this kind of species is stabilized to a lower extent on metal dispersed on alumina as compared with their silica-supported analogues under the same conditions (5). These species have been attributed to isolated carbon atoms adsorbed in hollow sites and bound to three or more surface metallic centers (33, 34); it has been found by nuclear magnetic resonance that there are only metal atoms in their first coordination sphere (35–38). Recent studies concerning the possibility of direct transformation of methane into higher hydrocarbons at moderate temperatures under nonoxidizing conditions indicate that this carbidic carbon is the one responsible for higher hydrocarbon formation after hydrogenation (39–41) or displacement by carbon monoxide adsorption (42). The location of these species on the metal surface makes of them the most reactive to be oxidized by the support OH groups. Thus, the amount of this type of carbon on a catalyst is dependent on the number of active surface sites and on the degree of hydration of the support. According to the lower density of hydroxyl groups on SiO_2 than on Al_2O_3, silica-supported metals have been found to stabilize a major amount of this kind of species as compared with alumina-supported analogues (5).

The less reactive C_β form, hydrogenatable at temperatures between 373 and 573 K, has been differentiated in two types of species, C_{β_1} and C_{β_2}, which differ in their mobility. They have been assigned to an amorphous structure in which carbon–carbon, carbon–metal, and hydrogen–carbon bonds are present (32). C_{β_1} species, hydrogenated between 373 and 450 K, might possibly be associated to surface carbonaceous species on the copper phase, as they were not found on the monometallic Rh/Al_2O_3 reference (5). Anderson *et al.* (31) found a maximum formation of C_2 species by hydrogenation of carbon deposits formed from methane decomposition on Cu/SiO_2 and $RhCu/SiO_2$ catalysts at a similar temperature (∼423 K). However, they appeared in lower amount than the carbidic carbon. Differences in the amounts obtained for C_α and C_{β_1} species are probably due to a support effect; i.e., the lower density of hydroxyl groups would limit the removal of carbidic carbon. In the range between 483 and 510 K a well-defined peak of CH_4 formation was obtained for all samples as for the monometallic Rh/Al_2O_3 reference, whose intensity increased gradually with the rhodium content in the catalyst (Fig. 3). The amount of C_{β_2} species accumulated was found to be directly related to the amount of rhodium atoms in the catalyst ($Rh/C_{500\,K}$ in Table 3). Tentatively, it might be related to interstitial carbonaceous species occluded in the rhodium phase with an approximated stoichiometry of Rh_3C. Solymosi and Cserényi (30) obtained TPH profiles of carbonaceous deposits formed from methane decomposition on Rh/SiO_2 and $RhCu/SiO_2$ catalysts at 573 K in which C_β species, hydrogenated between 450 and 550 K, also showed a direct proportionality between their peak intensity and the rhodium loading in each catalyst. They also observed, according to our results, an increment in the hydrogenation temperature of the C_{β_2} species on bimetallic samples when the copper amount was increased.

The less reactive form, C_γ carbon, has been usually assigned to a graphitic structure formed by groups of rings of six carbon atoms and probably located at the support surface (32), as previously postulated due to the high amount of methane converted during the TPSR experiment. The transformation of the most reactive species into the graphitic ones seems to be an irreversible process that would depend on the rate of surface and bulk diffusion of species through the metal–support interface. The temperature of reaction is, as suggested by Koerts *et al.* (32), an important parameter in the aging of these carbon species, which finally would determine the rate of all migration processes.

Reforming of Methane with Carbon Dioxide

The influence of the support on the catalytic activity of the active metal (Rh) is also clear from the results obtained for the reforming of methane with carbon dioxide. Firstly, catalytic activity of Rh/Al_2O_3, in terms of turnover numbers, has been found to exceed by an order of magnitude the level reached on the silica-supported sample (Table 4). Secondly, Rh/Al_2O_3 exhibits an excellent stability under reaction conditions at 823 K while its Rh/SiO_2 analogue undergoes a rapid deactivation, being almost completely inactive within 3 h.

In general, good stability properties have been found for rhodium-based systems applied to the reforming of methane with carbon dioxide, especially when the systems are alumina supported (3, 4, 7, 43). Silica-supported catalysts have usually shown a good stability for the reaction of $CH_4 + CO_2$, though in these cases the reaction tests have been performed at extreme temperatures: close to 673 K, at which the reaction starts (8), or above 923 K (7, 8, 28). Previous testing of these two catalysts in the reaction of CH_4 and CO_2 revealed for both of them a good stability at low (723 K) and high temperatures (1023 K), showing no deactivation by sintering or by carbon deposition (8). The different behavior shown by Rh/SiO_2 depending on the reaction temperature can be explained by considering that, at low temperatures, the activation of methane on rhodium is favored as compared with that of carbon dioxide but, due to the low level of conversion, carbon deposition on rhodium for the silica-supported sample is probably a slow process. In the high temperature range, the activation of carbon dioxide on rhodium is more effective and thus avoids the formation of carbon deposits, which are oxidized to carbon monoxide. At moderate temperatures, like the one used in the present study (823 K), the conditions of a relatively high conversion of methane and slow carbon dioxide activation concur, leading to a fast deactivation by carbon deposition. Thus, for Rh/SiO_2, the reaction temperature seems to be a key parameter for its stability toward carbon deposition. In agreement with our results, Lercher *et al.* (44) found for a silica-supported rhodium catalyst a strong deactivation process under reaction conditions at 873 K, while alumina- and zirconia-supported samples proved to be very stable under the same conditions.

In the case of rhodium-based catalysts, the CO_2 activation process has been frequently proposed as the rate-determining step for the dry reforming of methane (6, 45). It is well known that methane is easily dissociated on the rhodium surface (46), in contrast with carbon dioxide, whose dissociation on rhodium, at least at low and moderate temperatures, is relatively slower (47). By considering that on Rh/SiO_2 the rate-determining step of the reaction is the adsorption and dissociation of CO_2 on the metal surface, the possibility of an alternative and more efficient way to activate this molecule would result in a substantial increase of the catalytic activity, as has been observed for the alumina-supported catalysts.

The contrasting behavior of Rh/SiO_2 and Rh/Al_2O_3 catalysts with regard to their activity and stability indicates a major effect of the support. Complementary spectroscopic studies connect these important differences to the carbon dioxide activation. Carbon dioxide has been found to dissociate on the rhodium phase on Rh/SiO_2, generating carbon monoxide and oxidizing simultaneously the metal to Rh_2O_3, as observed by XANES and DRIFT spectroscopies. Linearly bound CO on Rh^0 centers became apparent under a carbon dioxide atmosphere indicating its dissociation, but the intensity of this band decreased with time until its disappearance. The oxidation of the rhodium phase has been found to be not only a surface process. Oxygen species from carbon dioxide dissociation diffuse to the bulk, and a Rh_2O_3-like phase is finally obtained, as revealed by the XANES Rh K-edge study (Figure 8). Similar results on silica-supported rhodium catalysts were reported by Wang and Au (28), who observed the initial activity for CO_2 decomposition to increase with the rhodium loading and with temperature.

A completely different situation was found for alumina-supported rhodium, in which the oxidation of the metallic phase was found to be much slower under a carbon dioxide atmosphere. Even after 15 min under those conditions the major part of the rhodium remained in metallic state as Rh^0 and no change in the XANES profile was observed (Fig. 8). DRIFT spectra obtained under flowing CO_2 showed the appearance of weak carbonyl bands on Rh^0 (Fig. 4), but they were observed to be constant with time, at least for 15 min, indicating that carbon dioxide activation on rhodium is a rather slow process on this catalyst. In addition, a broad feature due to alumina-adsorbed carbonates became apparent. The admission of methane in the feed caused this band to be partly transformed into formate adspecies with a simultaneous intensity increase of the bands due to the surface hydroxyl groups on alumina.

Formate species have been frequently considered as byproducts in this reaction as result of their formation on the alumina under flowing carbon monoxide, according to the equilibrium $OH^-_{(s)} + CO_{(g)} \Leftrightarrow HCO^-_{2(s)}$. However, it has been shown that the adsorption of carbon monoxide on the alumina and its reaction with the surface OH^- groups to yield HCO_2^- adsorbed species is practically negligible at temperatures as low as 523 K (Figure 7). The equilibrium between gas-phase carbon monoxide and adsorbed formate species on the alumina is displaced toward the reverse reaction when the temperature is increased. When CH_4 and CO_2 are fed together, formate species are generated from CO_3^{2-} hydrogenation on the alumina with simultaneous liberation of OH^- groups on the alumina surface (bands at ca. 3550 cm^{-1}) according to $CO^{2-}_{3(s)} + 2H_{(s)} \Leftrightarrow HCO^-_{2(s)} + OH^-_{(s)}$. Due to the high reaction temperature, these formate species are finally decomposed into CO and OH^- groups, as previously proposed. The continuous regeneration of surface hydroxyls contributes to maintain a high degree of hydration of the support, which has been shown to have a beneficial effect in the removal of carbonaceous species from the rhodium surface and, therefore, in the maintenance of the catalytic activity. According to this, a bifunctional mechanism is proposed for the reforming of methane with carbon dioxide on the alumina-supported rhodium catalyst: methane is activated on the metal phase while carbon dioxide is activated on the support. Similar conclusions have been reached for alumina-supported ruthenium catalysts (13, 14).

This bifunctional mechanism, in which two types of active centers are involved in the reaction pathway, leads us to propose two possibilities regarding their relative location. A first possibility would be to consider their concentration at the metal–support interface, allowing a direct exchange of species in order to close the balance between the individual processes of activation of each of the reactants. In this case, the addition of a nonactive metal, such as copper, would gradually reduce the number of sites of rhodium in direct contact with the support, particularly whether an alloyed phase is formed. Therefore, a decrease of activity would be observed as compared with the monometallic alumina-supported rhodium catalyst. A second option would be to suppose that these sites are separated from one another. Thus, active centers for methane activation would be located on the rhodium particles surface and sites for CO_2 activation would be spread on the alumina surface. Considering only this latter situation, the addition of copper independently of the presence of alloyed or unalloyed phases would not have a significant effect on the level of conversion reached. The results obtained support consequently this latter option. Catalytic activity tests showed that the activity per surface rhodium site does not vary significantly on bimetallic samples as compared with the alumina-supported rhodium catalyst (Table 4). In addition, by considering the distinct surface structure for the series of $RhCu/Al_2O_3$ catalysts, which have been thoroughly characterized (16, 17), the negligible effect of copper addition on rhodium activity indicates that the reforming of methane with carbon dioxide is not a structure-sensitive reaction.

In contrast, the rate of deactivation is larger on these bimetallic samples as compared with Rh/Al_2O_3. This effect is probably due to the increased difficulty in OH migration through the rhodium–alumina interface in the presence of copper. A thorough analysis shows that alloyed samples ($0.05RhCu/Al_2O_3$ and $0.14RhCu/Al_2O_3$) suffer deactivation to a lower extent than nonalloyed samples, a fact that can be connected with the larger accumulation of carbon species (C_{β_1}) in the copper component of the catalyst. This seems to suggest that the nature of the copper species present at the surface of the Rh particles also has an influence in this process. The mentioned lower accessibility of the hydroxyl groups to the rhodium phase would therefore limit to a certain extent the removal of carbonaceous adspecies from the metallic surface and decrease the stability of the reaction, leading to a slight but continuous deactivation of the catalysts. However, it must be taken into account that, even in the presence of copper, the degree of deactivation observed is much lower than the one observed for the silica-supported catalyst. The results presented here corroborate those recently reported by Stagg *et al.* on bimetallic Pt–Sn/SiO_2 and Pt–Sn/ZrO_2 catalyst (48, 49). They have found that the addition of Sn to Pt/SiO_2 reduces carbon deposition under the same reaction conditions and improves the stability of the reaction by partially inhibiting the decomposition of methane. In contrast, for Pt/ZrO_2, for which a bifunctional mechanism is also proposed, they observed a decrease of activity and stability when Sn was added to the catalyst. This has been attributed to the disruption of the interaction between Pt and ZrO_2, which leads to an imbalance between the rates of methane decomposition and the removal of carbonaceous deposits by oxygen species resulting from the carbon dioxide activation on the zirconia surface.

CONCLUSIONS

The addition of an inactive metal for the activation of methane, such as copper, to the Rh/Al_2O_3 system, which is very active for methane activation and for its reforming with carbon dioxide, has made possible to evaluate the role of the metal–support interface in this kind of catalysts, for which a bifunctional mechanism has been proposed. The experiments presented here indicate that this interfacial zone plays a key role in the chemistry of these reactions for alumina-supported catalysts. The surface diffusion of species through this metal–support interface makes possible to maintain an equilibrium between the activation of carbon dioxide in the alumina surface and the methane dehydrogenation reaction on rhodium, avoiding the accumulation of carbon deposits and the subsequent catalyst deactivation. The addition of copper limits to a certain extent the diffusion of these species between the support and the metal. Thus, a decreased stability has been observed on $RhCu/Al_2O_3$ catalysts in comparison with the Rh/Al_2O_3 system, which exhibits an excellent maintenance of its catalytic activity. However, the deactivation observed for the bimetallic samples is not so pronounced as in the case in which both reactants, methane and carbon dioxide, are activated on the rhodium surface, as found for the Rh/SiO_2 catalyst. No effect of the copper has been found on initial catalytic activity for the dry reforming of methane per surface rhodium site, not even in those catalysts with lower Rh/Cu ratios, in which interfacial sites will be mainly occupied by copper. The dry reforming of methane has been found consequently to be structure insensitive and to depend on the number of surface-exposed sites, not only on those located at the metal–support interface.

ACKNOWLEDGMENTS

This work was supported by CICYT, Spain, under Project MAT96-0859-CO2-02. P.F.A. acknowledges a scholarship grant from the Comunidad de Madrid, Spain. The DRIFTS measurements were carried out in collaboration with Dr. J. A. Anderson at the University of Dundee. M.F.G. thanks the Spanish Ministerio de Educación y Cultura for a postdoctoral contract.

REFERENCES

1. Bradford, M. C. J., and Vannice, M. A., *Catal. Rev.-Sci. Eng.* **41**, 1 (1999).
2. Edwards, J. H., *Catal. Today* **23**, 59 (1995).
3. Richardson, J. T., and Paritpayadar, S. A., *Appl. Catal.* **61**, 293 (1990).
4. Erdöhelyi, A., Cserényi, J., and Solymosi, F., *J. Catal.* **141**, 287 (1993).
5. Ferreira-Aparicio, P., Rodríguez-Ramos, I., and Guerrero-Ruiz, A., *Appl. Catal. A* **148**, 343 (1997).
6. Nakamura, J., Aikawa, K., Sato, K., and Uchijima, T., *Catal. Lett.* **25**, 265 (1994).
7. Zhang, Z. L., Tsipouriari, V. A., Efstathiou, A. M., and Verykios, X. E., *J. Catal.* **158**, 51 (1996).
8. Ferreira-Aparicio, P., Guerrero-Ruiz, A., and Rodríguez-Ramos, I., *Appl. Catal. A* **170**, 177 (1998).
9. Bitter, J. H., Seshan, K., and Lercher, J. A., *J. Catal.* **171**, 279 (1997).
10. van Keulen, A. N. J., Seshan, K., Hoebink, J. H. B. J., and Ross, J. R. H., *J. Catal.* **166**, 306 (1997).
11. Bradford, M. C. J., and Vannice, M. A., *J. Catal.* **173**, 157 (1998).
12. Bradford, M. C. J., and Vannice, M. A., *Appl. Catal. A* **142**, 97 (1996).
13. Ferreira-Aparicio, P., Márquez-Alvarez, C., Rodríguez-Ramos, I., Schuurman, Y., Guerrero-Ruiz, A., and Mirodatos, C., *J. Catal.* **184**, 202 (1999).
14. Ferreira-Aparicio, P., Rodríguez-Ramos, I., Anderson, J. A., and Guerrero-Ruiz, A., submitted for publication.
15. Liao, M. S., and Zhang, Q.-E., *J. Mol. Catal. A: Chem.* **136**, 185 (1998).
16. Ferreira-Aparicio, P., Bachiller Baeza, B., Rodríguez-Ramos, I., Guerrero-Ruiz, A., and Fernández-García, M., *Catal. Lett.* **49**, 163 (1997).
17. Fernández-García, M., Martínez-Arias, A., Rodríguez-Ramos, I., Ferreira-Aparicio, P., and Guerrero-Ruiz, A., *Langmuir* **15**, 5295 (1999).
18. Busca, G., and Lorenzelli, V., *Mater. Chem.* **7**, 89 (1982).
19. Kiselev, A. V., and Lygin, V. Y., *in* "Infrared Spectra of Surface Compounds." Wiley, New York, 1975.

20. Schubert, M. M., Gasteiger, H. A., and Behm, R. J., *J. Catal.* **172**, 256 (1997).
21. Kantschewa, M., Albano, E., Ertl, E. V., and Knözinger, H., *Appl. Catal.* **8**, 71 (1983).
22. Buyevskaya, O. V., Wolf, D., and Baerns, M., *Catal. Lett.* **29**, 249 (1994).
23. Walter, K., Buyevskaya, O. V., Wolf, D., and Baerns, M., *Catal. Lett.* **29**, 261 (1994).
24. Efstathiou, A. M., Kladi, A., Tsipouriari, V. A., and Verykios, X. E., *J. Catal.* **158**, 154 (1996).
25. Anderson, J. A., and Solymosi, F., *J. Chem. Soc., Faraday Trans.* **87**, 3435 (1991).
26. Fischer, J. A., and Bell, A. T., *J. Catal.* **162**, 54 (1996).
27. Wang, D., Dewaele, O., and Froment, G. F., *J. Mol. Catal. A: Chem.* **136**, 301 (1998).
28. Wang, H. Y., and Au, C. T., *Appl. Catal. A* **155**, 239 (1997).
29. Koranne, M. M., and Goodman, D. W., *Catal. Lett.* **30**, 219 (1995).
30. Solymosi, F., and Cserényi, C., *Catal. Lett.* **34**, 343 (1995).
31. Anderson, J. A., Rochester, C. H., and Wang, Z., *J. Mol. Catal.* **139**, 1381 (1998).
32. Koerts, T., Deelen, M. J. A. G., and van Santen, R. A., *J. Catal.* **138**, 101 (1992).
33. De Kooster, A., and van Santen, R. A., *J. Catal.* **127**, 141 (1991).
34. Koerts, T., and van Santen, R. A., *J. Mol. Catal.* **70**, 119 (1991).
35. Duncan, T. M., Winslow, P., and Bell, A., *Chem. Phys. Lett.* **102**, 163 (1983).
36. Winslow, P., and Bell, A., *J. Catal.* **86**, 158 (1984).
37. Winslow, P., and Bell, A., *J. Catal.* **91**, 142 (1985).
38. Duncan, T. M., Winslow, P., and Bell, A., *J. Catal.* **93**, 1 (1985).
39. Koerts, T., and van Santen, R. A., *J. Chem. Soc., Chem. Commun.* 1281 (1991).
40. Belgued, M., Amariglio, H., Paréja, P., Amariglio, A., and Saint Just, J., *Catal. Today* **13**, 437 (1992).
41. Cheikhi, N., Ziyad, M., Coudourier, G., and Vedrine, J., *Appl. Catal. A* **118**, 187 (1994).
42. Amariglio, H., Belgued, M., Paréja, P., and Amariglio, A., *Catal. Lett.* **31**, 19 (1995).
43. Mark, M. F., and Maier, W. F., *J. Catal.* **164**, 122 (1996).
44. Bitter, J. H., Seshan, K., and Lercher, J. A., *J. Catal.* **176**, 93 (1998).
45. Efstathiou, A. M., Kladi, A., Tsipouriari, V. A., and Verykios, X. E., *J. Catal.* **158**, 154 (1996).
46. Goodman, D. W., Peebles, D. E., and White, J. M., *Surf. Sci.* **140**, L239 (1984).
47. Solymosi, F., *J. Mol. Catal.* **65**, 337 (1991).
48. Stagg, S. M., and Resasco, D. E., *Stud. Surf. Sci. Catal.* **111**, 543 (1997).
49. Stagg, S. M., Romeo, E., Padro, C., and Resasco, D. E., *J. Catal.* **178**, 137 (1998).